Volume 11
Number 3
7 February 2023
Pages 693-1080

Biomaterials Science

rsc.li/biomaterials-science

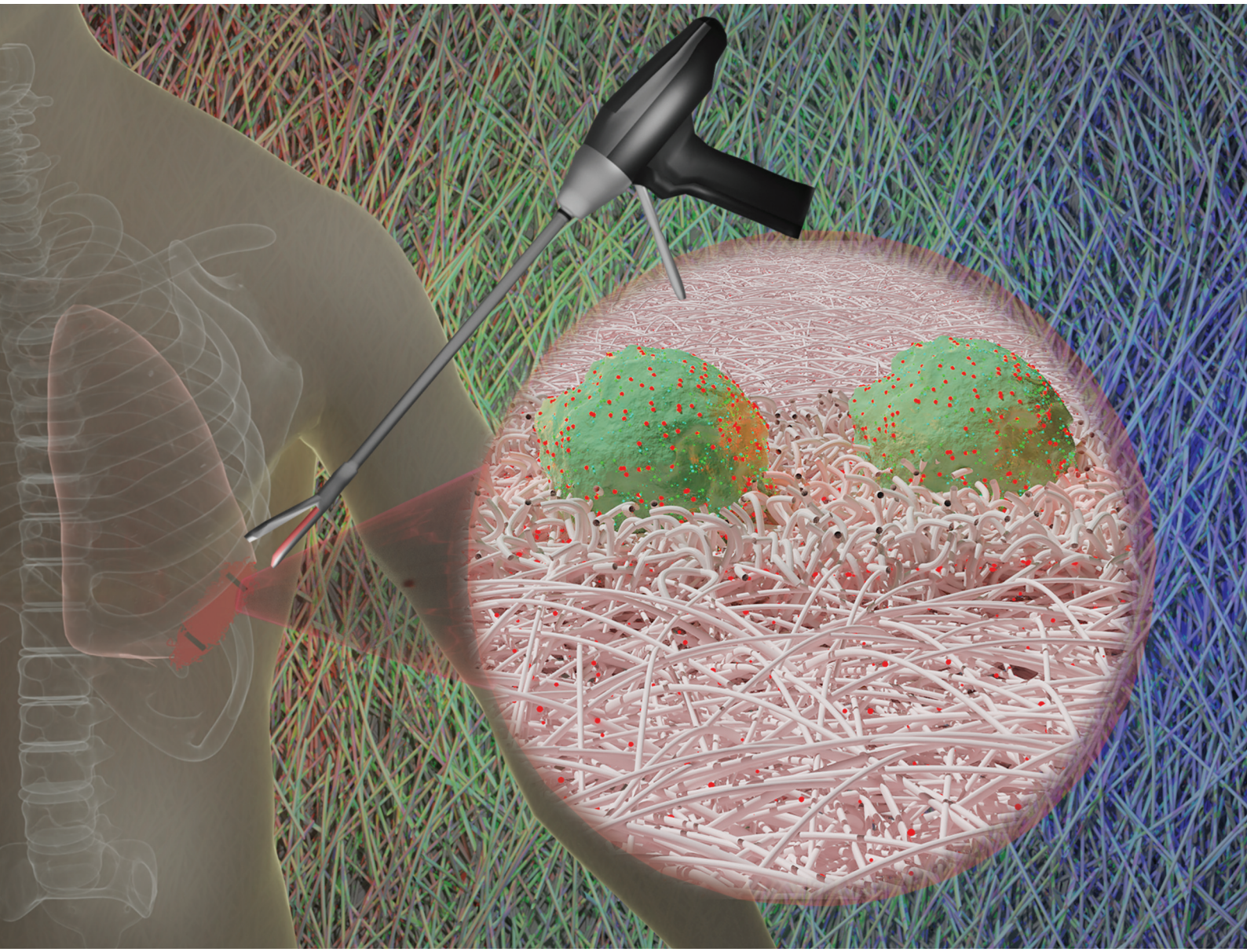

ISSN 2047-4849

ROYAL SOCIETY OF CHEMISTRY

PAPER
Mark W. Grinstaff, Amitav Sanyal *et al.*
pH-Responsive nanofiber buttresses as local drug delivery devices

European Society for Biomaterials

Biomaterials Science

ROYAL SOCIETY OF CHEMISTRY

PAPER

View Article Online
View Journal | View Issue

Cite this: *Biomater. Sci.*, 2023, **11**, 813

pH-Responsive nanofiber buttresses as local drug delivery devices†

Ismail Altinbasak, [a] Salli Kocak,[a] Aaron H. Colby,[c] Yasin Alp,[a] Rana Sanyal,[a,b] Mark W. Grinstaff *[c,d] and Amitav Sanyal *[a,b]

Electrospun nanofibers are a 3D scaffold of choice for many drug delivery devices due to their high surface area, significant capacity for drug payload, ease of *in situ* placement, and scalable manufacture. Herein, we report the synthesis of polymeric, pH-responsive nanofiber buttresses *via* electrospinning. The homopolymer is comprised of an acrylic backbone with acid-sensitive, hydrolyzable, trimethoxybenzaldehyde-protected side chains that lead to buttress transformation from a hydrophobic to a hydrophilic state under physiologically relevant pH conditions (*e.g.*, extracellular tumor environment with pH = 6.5). Hydrolysis of the side chains leads to an increase in fiber diameter from approximately 350 to 900 nm and the release of the encapsulated drug cargo. *In vitro* drug release profiles demonstrate that significantly more drug is released at pH 5.5 compared to pH 7.4, thereby limiting the release to the target site, with docetaxel releasing over 20 days and doxorubicin over 7 days. Drug burst release, defined as >50% within 24 hours, does not occur at either pH or with either drug. Drug-loaded buttresses preserve drug activity and are cytotoxic to multiple human cancer lines, including breast and lung. Important to their potential application in surgical applications, the tensile strength of the buttresses is 6.3 kPa and, though weaker than commercially available buttresses, they provide sufficient flexibility and mechanical integrity to serve as buttressing materials *via* the application with a conventional surgical cutting stapler.

Received 30th July 2022,
Accepted 8th November 2022

DOI: 10.1039/d2bm01199a

rsc.li/biomaterials-science

Introduction

Polymeric materials that undergo transformation of their chemical, physical, and/or mechanical properties in response to environmental changes are of significant interest in myriad biomedical applications.[1–5] Light,[6–8] temperature,[9] pH,[10] magnetism[11] or exposure to a specific biological molecule are examples of relevant stimuli.[12–14] Of these, pH is one of the most studied as differences in pH between neighboring tissues (*e.g.*, stomach *vs.* intestine), within the extracellular matrix of tumors (pH 6.5) and within the intracellular compartments of cells (pH 5) allow for accurate triggering of systems based on physiological location.[15–18] Common form factors for such stimuli-responsive polymer materials include: micro- and nano-particles,[19,20] hydrogels,[21,22] surfaces and coatings,[23] and nanofibers.[24] Electrospun nanofibers are particularly advantageous in drug delivery applications due to their high surface area to volume ratio, their capacity for both high as well as efficient drug-loading, their functionalizable surface chemistry, and their ease of *in situ* placement at a target site during surgical procedures.[25–32] Furthermore, electrospinning is a robust and scalable industrial process, thereby enabling ready access to large-scale production of such materials for clinical applications.[33,34]

Stimuli-responsive nanofibers, and their corresponding macroscopic polymer buttresses, have been designed to leverage changes in temperature[35] or pH,[36] the application of light[37] or ultrasound,[38] and even increases in oxidative stress[39] to trigger drug release. In general, stimuli such as light, ultrasound, and temperature are pragmatic only for on-demand drug release over relatively short periods of time and are restricted to tissue locations accessible to these externally applied stimuli.[40,41] On the other hand, endogenous stimuli, such as changes in local redox or pH, may occur over longer periods, thereby affording the opportunity to control drug release over extended periods of time.[42,43] For example, Li and coworkers reported pH-responsive nanofibers composed of triblock copolymers comprised of poly(D,L-lactide) as terminal

[a]*Department of Chemistry, Bogazici University, Bebek, Istanbul 34342, Turkey. E-mail: amitav.sanyal@boun.edu.tr*
[b]*Center for Life Sciences and Technologies, Bogazici University, Bebek, Istanbul 34342, Turkey*
[c]*Boston University, Department of Biomedical Engineering, Boston, MA, USA. E-mail: mgrin@bu.edu*
[d]*Boston University, Department of Chemistry, Boston, MA, USA*
† Electronic supplementary information (ESI) available. See DOI: https://doi.org/10.1039/d2bm01199a

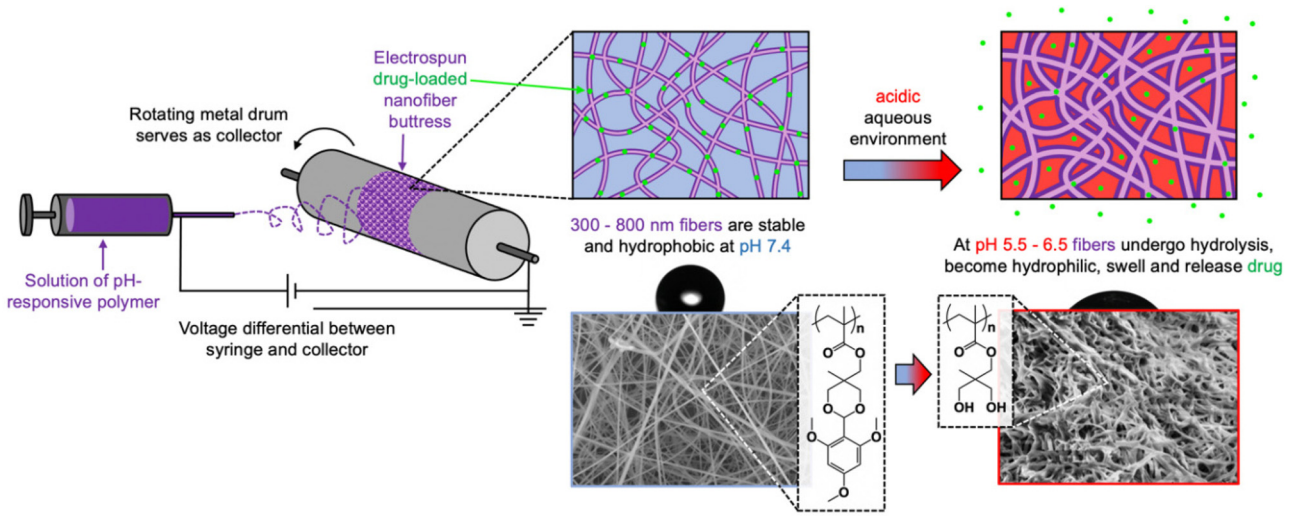

Scheme 1 Illustration of the fabrication and application of pH-responsive nanofiber buttresses. The hydrophobic group of nanofiber is cleaved at lower pH. This transformation from hydrophobic to hydrophilic results in swelling and drug release from the nanofiber buttresses.

blocks and an acetal-linked poly(ethylene glycol) central block.[44] The fiber morphology of this system gradually changes after incubation in pH 7.4, 5.6, and 4.0 buffer solutions with eventual loss of the fiber structure. Entrapped paracetamol ($\log P$ = 0.46) releases from the nanofibers over 120 hours in a pH-dependent manner, with the fastest release occurring in a pH = 4 buffer. However, a limitation of this system is significant passive release, regardless of pH, leading to rapid emptying of the delivery vehicle within a matter of days.

As an alternative to a hydrolytic polymer backbone, which undergoes degradation to release its drug payload, we employ a polymer with a non-hydrolyzable methacrylate backbone with acid-labile side chains that undergo cleavage under mildly acidic conditions thereby resulting in an overall change in the polymer composition from hydrophobic to hydrophilic. Due to the presence of the methacrylate backbone, the fibers can maintain their structure, rather than degrading/dissolving into solution, while swelling and, subsequently, increasing in diameter. The 2,4,6-trimethoxybenzaldehyde moiety, reported by Fréchet[45] and Grinstaff,[46,47] is one example of an acid-labile protecting group that is, itself, hydrophobic in nature and, upon cleavage, can afford two hydrophilic hydroxyl groups. For example, Fréchet-type amphiphilic dendrons terminated with 2,4,6-trimethoxy benzaldehyde acetal groups assemble into micelles and encapsulate doxorubicin.[45] Hydrolysis of the acetal group at pH 6 results in release of doxorubicin and disruption of the micelle. Grinstaff and coworkers describe a methacrylate-based diol monomer protected with a 2,4,6-trimethoxybenzaldehyde moiety for preparing polymeric nanoparticles *via* a mini-emulsion polymerization technique. In their initial state, the 100 nm particles are hydrophobic but when exposed to a mildly acidic environment of pH 5–6, they swell in diameter to 1000 nm; as a result of this swelling behavior, they are termed "expansile nanoparticles" (eNPs).[47] Drug loaded eNPs are readily taken up by multiple cancer cells[48–51] and localize with high specificity to mesothelioma, ovarian and pancreatic tumors following intraperitoneal injection.[52,53] Improved outcomes have been shown in xenograft murine models of pancreatic cancer,[46] breast cancer,[49] mesothelioma,[54] and ovarian cancer.[55]

Herein, we repurposed this eNP polymer to create drug-loaded nanofibers that can be formed into surgical buttresses to enable site-specific, pH-controlled drug release (Scheme 1). We report the free radical polymerization of a 2,4,6-trimethoxybenzaldehyde-containing methacrylate monomer and the subsequent fabrication of electrospun buttresses using this polymer. Both hydrophilic (doxorubicin) and hydrophobic (docetaxel) drugs are loaded into the nanofibers as characterized by scanning electron microscopy (SEM), and confocal microscopy. The nanofibers retain their shape but increase in size while swelling in a mildly acidic buffer solution. Docetaxel and doxorubicin release from the nanofiber buttresses is negligible at neutral pH and occurs more rapidly in a mildly acidic buffer solution. Released drug is still active and cytotoxic to lung (NCI-H460, A549) and breast cancer (MDA-MB-231) cells.

Experimental section

Materials

2,4,6-Trimethoxybenzaldehyde was purchased from Acros Organics. 1,1,1-Tris(hydroxymethyl)ethane was purchased from Alfa Aesar. Methacryloyl chloride was purchased from Sigma Aldrich. The organic solvents dichloromethane, hexane, dimethylformamide, and methanol were analytical grade and purchased from Sigma Aldrich. Doxorubicin hydrochloride and fluorescein amine, isomer I were purchased from Sigma Aldrich. These chemicals were used without further purifi-

cation. MDA-MB-231, A549, and NCI-H460 cell lines were purchased from ATCC (LGC Standards, Germany) and grown according to the culture method requirements of the manufacturer. Cells were incubated at 37 °C in a humidified atmosphere of 5% CO_2. Cytotoxicity experiments were performed with a plate reader (Multiscan FC, Thermo Scientific, USA) and Cell Counting Kit8 (CCK-8, Fluka) obtained from Sigma-Aldrich. The monomer was prepared according to previously reported literature.[47,56]

Synthesis of pH-responsive polymer

Synthesis of homopolymer has been reported by Grinstaff and coworkers previously.[56] Briefly, the monomer (0.55 g, 1.5 mmol, 150 equiv.), AIBN (0.16 mg, 0.001 mmol, 0.1 equiv.), and the solvent dimethylacetamide (0.41 mL) were added to a round bottom flask. The solution was purged with N_2 gas for 30 minutes. After 30 minutes, the solution was put in an oil bath at 80 °C for two hours. To purify the highly-dense polymer solution, the resulting mixture was diluted with 10 mL of dichloromethane and precipitated in cold ether. Polymers with 140 and 320 kDa (M_w) were characterized by size exclusion chromatography using Shimadzu PSS-SDV (length/ID 8 × 300 nm, 10 μm particle size) calibrated with polymethylmethacrylate standards using a refractive index detector. The structure of the polymer was confirmed by ^{1}H NMR.

Fabrication and characterization of drug-loaded nanofibers

For a typical experiment, a polymer solution of 17 wt% and drug (docetaxel or doxorubicin) 1 wt%, and fluorescein amine 1 wt% in 1 : 1 (v/v) DMF : THF solvent mixture was prepared and the solution was stirred for 24 h at room temperature. Clear polymer/drug solution was electrospun using a syringe pump (KD Scientific 101) at a constant flow rate (0.005 mL min^{-1}) with a 1 mL syringe fitted with a 14-gauge needle with 15 kV. The tip to collector distance was maintained at 15 cm during the electrospinning process. Fibers were collected on a rotating aluminum drum for further use. To calculate the drug loading efficiency, the nanofiber buttress was dissolved in dichloromethane and the solution was precipitated in methanol and the aliquot was analyzed *via* liquid chromatography-mass spectrometry (LC-MS) using an LC-MS-2020-Mass Spectrometer System (Shimadzu, Japan). To calculate the fluorescein amine loading efficiency, the aliquot was analyzed *via* UV-vis spectrophotometry using a Cary Varian UV–Vis spectrometer (Santa Clara, CA). Surface morphology was analyzed with scanning electron microscopy using a JEOL NeoScope JCM-5000. Distribution of doxorubicin in the nanofiber buttress was evaluated using a confocal laser scanning microscope (Leica TCS SP5). The static contact angle of a water droplet on electrospun nanofiber buttresses was measured under open-air conditions. Approximately 25 μL of deionized water was dropped on the surface and images were taken *via* an integrated digital camera. The software of the camera provides contact angle measurements once the liquid is dispensed. Freshly prepared nanofiber buttresses incubated in water and buffer solutions with different incubation times were used to measure contact angles after they were washed with distilled water to remove residual salt remaining from the buffer solutions used for incubation. Mechanical testing of the drug-loaded buttresses was performed using an Instron 5944 Microtester with 1 cm × 10 cm shaped rectangles secured at each end with binder clips and a nominal strain rate of 1 mm s^{-1}.

Hydrolysis of nanofibers

Hydrolysis studies were performed in phosphate-buffered saline (PBS) (1 mL, pH 7.4), phosphate buffer (1 mL, pH 6.5), or acetate buffer (1 mL pH 5.5) in an environmentally controlled thermal shaker at 37 °C with samples shaking at 100 rpm. The amount of 2,4,6-trimethoxybenzaldehyde protecting group released at each time point was quantified *via* LC-MS.

In vitro drug and fluorescein-amine release from nanofibers

Studies were performed in PBS (1 mL, pH 7.4), phosphate buffer (1 mL, pH 6.5), or acetate buffer (1 mL pH 5.5) in an environmentally controlled thermal shaker at 37 °C with samples shaking at 100 rpm. Additionally, drug release studies were also performed in 2 different cell culture media (RPMI-HEPES) at pH 7.4 and pH 6.5. The amount of drug released into the solutions at each time point was monitored *via* LC-MS/MS (Shimadzu triple quadrupole 8040) and the amount of fluorescein amine released in solution was monitored *via* UV-vis spectrophotometer.

Cytotoxicity assay

Cytotoxicity of the drug-loaded buttresses was evaluated using a CCK-8 viability assay on MDA-MB-231, A549, and NCI-H460 cells. Cells were seeded into 96-well plates (6000, 7000, 10 000 cells per well, respectively) in quadruplicate and incubated at 37 °C overnight to allow for complete adherence. For free drug treatments, the doxorubicin stock solution was prepared as 10^{-3} M (with 2.5% DMSO) to ensure complete dissolution of free doxorubicin. Serial dilutions were made from stock solution (10^{-3} M) using cell media and the final DMSO concentration in each well was kept below 0.5% (v/v). Nanofibers with doxorubicin (1 mg mL^{-1}) and empty nanofibers for control (1 mg mL^{-1}) were incubated in media (pH 6.5 and pH 7.4) at 37 °C for 5 days. For aliquots from drug loaded nanofibers, one to five dilutions were made with fresh media before adding the solution to cells. For aliquots from control nanofibers, one to ten serial dilution were made with fresh media before addition to the cells. After 48 h, CCK-8 solution (0.1%) was added to each well. After two hours of incubation, the absorbance values were measured with a plate reader (Multiscan FC, Thermo Scientific, USA) at 450 nm. Cell viability of treated cells was determined according to the percentage of control cells (cell media only). Results were calculated using GraphPad Prism software using a nonlinear regression mode.

Results and discussion

Synthesis of pH-responsive polymer

To manufacture a pH-responsive polymer buttress drug delivery system, we first synthesized an acid-labile methacrylate monomer for subsequent polymerization and buttress fabrication. Specifically, 5-methyl-2-(2,4,6-trimethoxyphenyl)-[1,3]-5-dioxanyl-methyl methacrylate, an acetal-containing pH-sensitive hydrophobic monomer obtained using 2,4,6-trimethoxybenzaldehyde as a building block was prepared. According to a previously reported protocol,[47,56] we reacted 2,4,6-trimethoxybenzaldehyde with 1,1,1-tris(hydroxymethyl)ethane to obtain an acetal-containing alcohol, which was coupled to methacryloyl chloride to yield the monomer in high yield and purity. Using this monomer, we performed a conventional free radical polymerization to obtain the polymers in good yield (90%) and high molecular weight. Specifically, the monomer was polymerized in the presence of varying amounts of AIBN at 80 °C for two hours in dimethylacetamide to afford polymers with weight average molecular weight of approximately 140 kDa and 320 kDa, with polydispersity index of 2.5 and 2.2, respectively, as determined using size exclusion chromatography (Fig. S1†). The chemical composition of the polymer was confirmed using ^{1}H NMR spectroscopy (Fig. S2†).

Fabrication of drug-loaded pH-responsive nanofibers

We fabricated nanofibers and corresponding buttresses *via* electrospinning. We targeted two different nanofiber diameters to determine whether smaller diameter nanofibers would release drug more rapidly due to an increase in the surface area to volume ratio.

Using polymers of molecular weights 140 kDa and 320 kDa, we obtained nanofibers with significantly different ($p < 0.0001$) diameters of 350 ± 64 and 800 ± 125 nm, respectively. We used a DMF/THF (1 : 1) solvent mixture, with a flow rate of 0.005 mL min^{-1}, and a 15 kV voltage potential between collector-needle at 15 cm to obtain bead-free, uniform nanofibers (Fig. 1a–d). Compounds (*e.g.*, doxorubicin, docetaxel or fluorescein amine) were loaded into the fibers by dissolving them in the DMF/THF solvent prior to electrospinning. The spatial distribution of doxorubicin was assessed *via* confocal laser microscopy and found to be relatively homogeneous (Fig. 1e). Loading efficiency of drugs within nanofibers was calculated by dissolving the fibers in a minimal amount of CH_2Cl_2, followed by removal of the polymer by precipitation in CH_3OH and centrifugation. The loading efficiencies of doxorubicin and docetaxel, were found to be 71%, and 64%, respectively, as quantified by LC-MS. The loading efficiency of fluorescein amine was determined as 27% using UV-vis spectroscopy.

pH-Responsiveness of nanofibers

To characterize the response of the nanofiber buttresses to pH changes, we measured their surface contact angle. Since acetal bonds are highly sensitive to low pH, they hydrolyze with release of the hydrophobic trimethoxybenzaldehyde groups with formation of hydrophilic diols along the polymer backbone (Fig. 2a). The contact angle of deionized water on a dry nanofiber buttress was approximately 140°, indicating the strongly hydrophobic

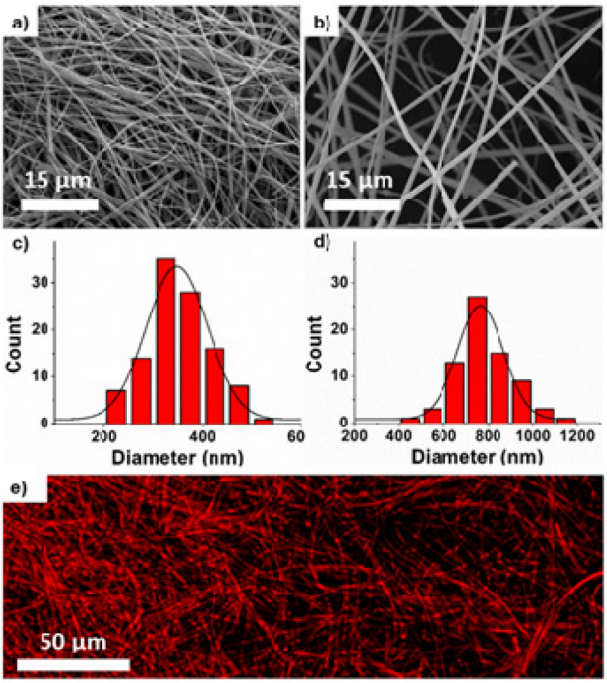

Fig. 1 SEM images of nanofibers with (a) 350 nm and (b) 800 nm diameters with their size distribution histograms, (c) and (d), respectively, and (e) representative confocal microscopy image of doxorubicin-loaded nanofibers.

nature of these materials (Fig. 2b). Incubating the nanofiber in water or PBS (pH 7.4) for up to 2 days did not result in major changes in contact angle (Fig. 2d). In contrast, when the nanofiber buttresses were immersed in an acidic buffer (pH 5.5), we observed a significant decrease in the contact angle to 107° after 3 hours with a further decrease to 60° after 6 hours (Fig. 2c). Over the next three days, the rate of change in contact angle did not decrease further, suggesting that most of the surface had already transformed from a hydrophobic to a hydrophilic state (Fig. 2e).

To further characterize this transformation and corroborate the contact angle findings, we measured the release kinetics of the trimethoxybenzaldehyde protecting group from the nanofiber buttress as a function of pH and time. As quantified by LC-MS, release of trimethoxybenzaldehyde from the buttress at pH 7.4 was minimal, with only 15% release after 28 days. In contrast, nearly 75% of the trimethoxybenzaldehyde was released at pH 5.5 over the same timeframe. To mimic the pH environment of tumor tissue, we repeated the study at a mildly acidic condition of pH 6.5. The release of trimethoxybenzaldehyde was more than 2-fold greater at pH 6.5 compared to the release in neutral pH, but slower than at pH 5.5 (Fig. 2f).

The increase in hydrophilicity of the polymer fibers was expected to result in swelling, manifest as an increase in average fiber diameter over time. Therefore, we used SEM to monitor the size of nanofibers incubated under various pH conditions. Nanofiber buttresses incubated in PBS for four weeks at 37 °C showed no significant change in fiber morphology or diameter (Fig. 3a–c).

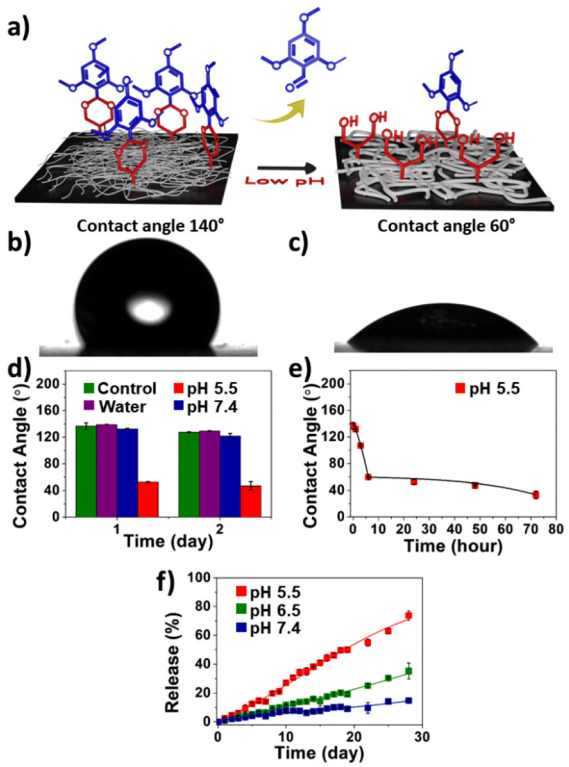

Fig. 2 (a) Schematic of pH-labile polymer cleavage and fiber swelling. Image of water droplet on (b) nanofiber buttress incubated in PBS or (c) on a nanofiber buttress incubated in pH 5.5 buffer. (d) Contact angle measurements of nanofiber buttresses incubated in different conditions (control = air). (e) Change in contact angle of nanofiber buttresses in an acidic buffer. (f) Release kinetics of trimethoxybenzaldehyde from nanofiber buttresses as a function of pH and time at 37 °C (N = 3).

In contrast, nanofiber buttresses incubated in pH 5.5 aqueous buffer over the same timeframe showed a three-fold increase in fiber diameter (Fig. 3d). Interestingly, by four weeks, the fibers began to lose their distinct shape and coalesce into larger, amorphous structures. This difference in morphology and increase in nanofiber diameter is consistent with hydrolysis and swelling of the polymer observed in other applications, such as with nanoparticles of the same material.[57]

Effect of fiber diameter on release rate of an encapsulated cargo

To evaluate the impact of fiber diameter on the release rate of an encapsulated small molecule cargo, we loaded the nanofibers with fluorescein amine. Fluorescein amine-loaded nanofiber buttresses with average diameters of 350 nm and 800 nm were immersed in pH 5.5 and pH 7.4 aqueous buffer and incubated in a thermal shaker at 100 rpm at 37 °C for nine days. Aliquots of release medium were taken daily and analyzed *via* UV-vis spectroscopy. As shown in Fig. 4, fiber diameter significantly impacted the release rate of fluorescein amine with 100% release from the 350 nm diameter fibers occurring within five days compared to only 30% release from the 800 nm diameter fibers over the same period. The 800 nm diameter fibers took fully nine days to release 100% of their cargo. This nearly two-fold difference in release rate is likely due to the increased surface area to volume ratio of the 350 nm fibers compared to the 800 nm fibers which leads to both faster hydrolysis of the pH-responsive polymer as well as ensuing release of cargo. A similar trend in fluorescein release based on nanofiber diameter was also observed at pH 7.4 (Fig. S3†). This is unsurprising as the influence of surface area to volume ratio (*i.e.*, that smaller fibers with greater surface

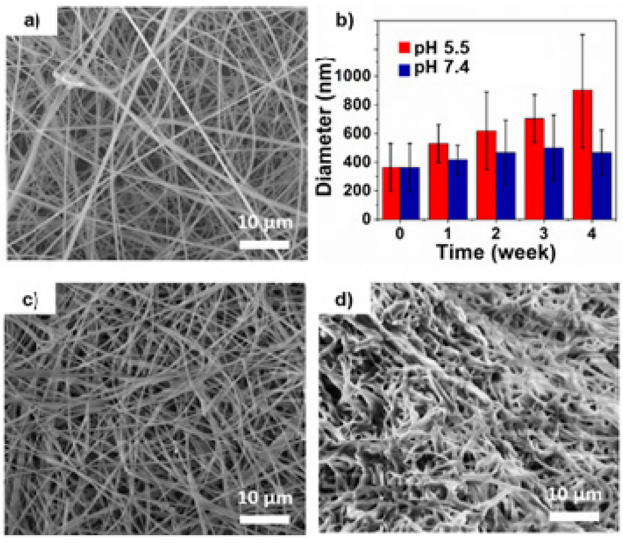

Fig. 3 (a) SEM image of nanofibers prior to incubation in aqueous solution. (b) Change in fiber diameter as a function of time and buffer pH (N = 3). (c) SEM image of nanofibers after incubation for four weeks in pH 7.4 PBS and (d) after four weeks in pH 5.5 aqueous buffer.

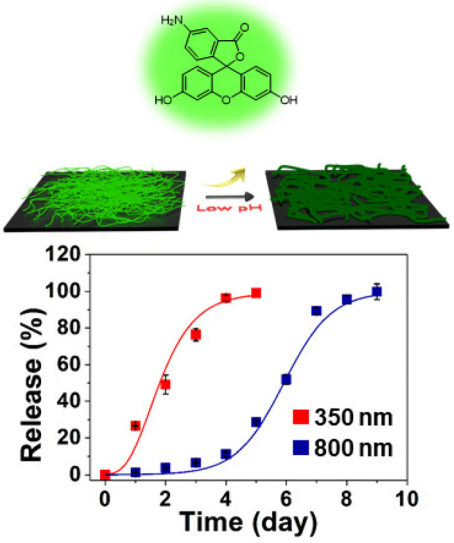

Fig. 4 The release of fluorescein amine from nanofiber buttresses as a function of fiber diameter and time while incubated in pH 5.5 aqueous buffer (N = 3).

area to volume ratios release faster) may be expected to be similar regardless of whether drug is merely "leaking" out at pH 7.4 or actively being released due to swelling at pH 5.5.

pH-Responsive drug release from the nanofibers

Due to the faster response time (*i.e.*, shorter lag between pH change and induction of significant drug release) of the smaller, 350 nm diameter fiber system, we chose to use these in subsequent studies evaluating the encapsulation and release of chemotherapeutic agents to shorten experimental duration of these studies and, therein, reduce potential confounding factors. We characterized the release of both of a hydrophilic drug (doxorubicin; $\log p$ = 1.3) and a hydrophobic drug (docetaxel; $\log p$ = 2.4) from the nanofiber buttresses incubated in both aqueous buffer solutions (pH 5.5 and 7.4) as well as cell culture media (RPMI-HEPES) adjusted to pH 7.4 and 6.5. Docetaxel did not release from the buttresses at pH 7.4 over eighteen days (Fig. 5a). In contrast, measurable release of docetaxel began after seven days of incubation at pH 5.5 with 100% release by day eighteen. Similar trends were observed with doxorubicin; however, the time scale of release was substantially shorter. At neutral pH, doxorubicin did not release from the buttresses. However, at pH 5.5, doxorubicin release began within 24 hours of incubation and reached 100% within six days (Fig. 5b). The faster rate of release of doxorubicin compared to docetaxel is to be expected based on its significantly more hydrophilic nature compared to docetaxel, which leads to greater affinity for the surrounding aqueous environment. Digital images of doxorubicin loaded nanofiber buttresses before and after the release at pH 5.5 (acetate buffer), and at pH 6.5 and 7.4 in RPMI-HEPES cell medium showed that while the fiber mat slowly dissolves at pH 5.5, it remains physically intact during this period at the higher pH's (Fig. S4†).

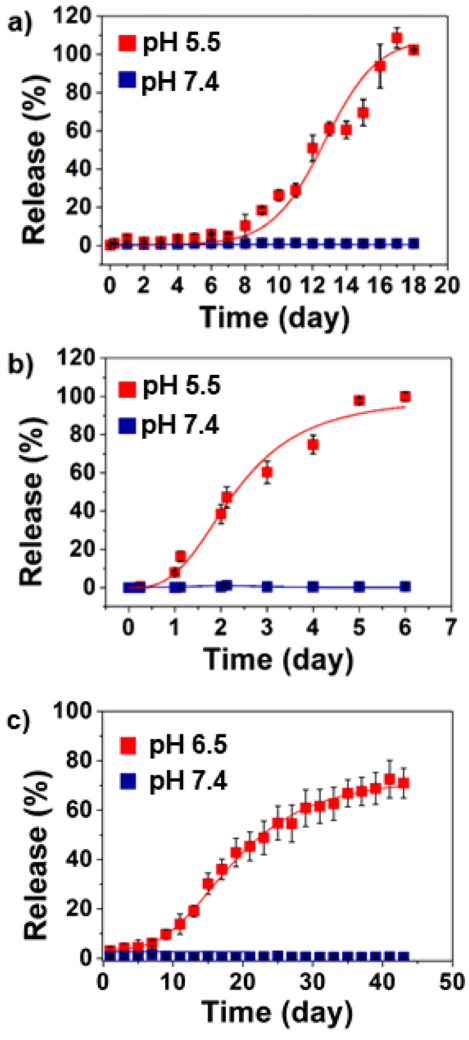

Fig. 5 Release of (a) docetaxel and (b) doxorubicin from nanofiber buttresses as a function of time and pH in aqueous buffer. (c) Release of doxorubicin from nanofiber buttresses as a function of time and pH in RPMI-HEPES media (all data $N \geq 3$).

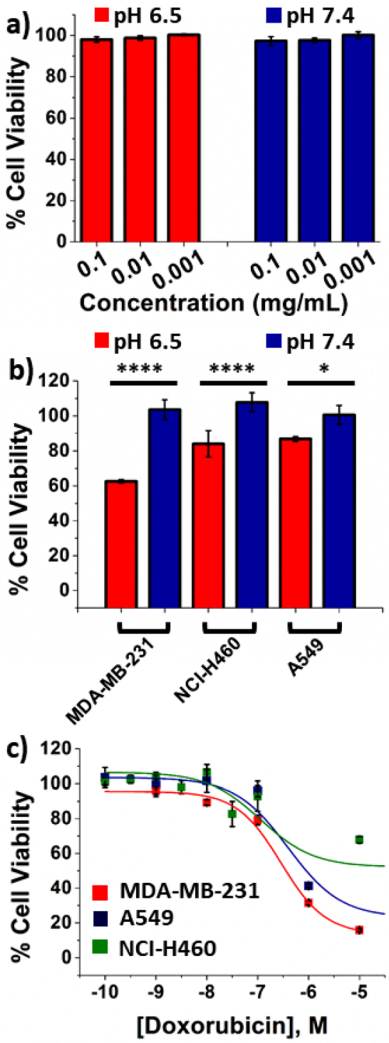

Fig. 6 (a) Cytotoxicity of supernatant from unloaded nanofibers incubated at pH 6.5 or 7.4 diluted and incubated with MDA-MB-231 cells. (b) Cytotoxicity of supernatant from doxorubicin-loaded nanofibers incubated at pH 6.5 or 7.4 diluted and incubated with MDA-MB-231, A549, and NCI-H460 cells. (c) Cytotoxicity of free doxorubicin on MDA-MB-231, A549, and NCI-H460 cells (all data $N \geq 3$).

Given the negligible release of doxorubicin at pH 7.4 over seven days, we performed an extended study in which doxorubicin release was monitored for four months under the same conditions as the previous study. Notably, the nanofibers retained the doxorubicin cargo without appreciable "leakage" (*i.e.*, unintended release at neutral pH) for the duration of the four-month study. Furthermore, extraction and quantification of the payload after four months demonstrated that the doxorubicin payload was preserved within the fibers without degradation (Fig. S5†).

Similarly, based upon the rapid release of doxorubicin observed at pH 5.5, we chose to evaluate its release rate at pH 6.5. This slightly higher, yet still mildly acidic, pH is physiologically relevant as it is a hallmark of the tumoral microenvironment[58,59] and a device implanted against the tumor bed may be expected to be exposed to these conditions. Compared to pH 5.5, doxorubicin release at pH 6.5 was slower, reaching approximately 13% release after two weeks. As before, no significant release was observed in pH 7.4 (Fig. S6†).

Lastly, in order to more accurately model physiological drug release conditions, we repeated the doxorubicin release studies in cell media (RPMI-HEPES), as opposed to simple aqueous buffers, adjusted to pH 6.5 and pH 7.4. Fig. 5c shows that the release profile of doxorubicin from nanofibers in cell culture was, again, pH-dependent. Sustained release of doxorubicin occurred at pH 6.5 with 70% of the payload being released by day forty-five. Negligible release occurred at pH 7.4 (2% over the same period). Notably, the release was significantly faster in media than in simple aqueous buffer (~25% *vs.* ~13% release over two weeks, respectively; Fig. 5c and Fig. S6†). This is likely the result of the presence of proteins in the media, which leads to faster wetting of the fibers and, hence, hydrolysis, as well as serving to increase the affinity of the drug for the sink.

In vitro cell viability studies

First, we assessed the cytotoxicity of unloaded nanofiber buttresses by immersing them in DMEM cell culture media at pH 7.4 and pH 6.5 for five days. This media was then serially diluted 10-, 100- or 1000-fold with fresh media and MDA-MB-231 breast cancer cells were incubated in these dilutions for two days. No cytotoxicity was observed from the unloaded buttresses (Fig. 6a). Furthermore, no significant cytotoxicity was observed when cells were incubated with the degradation product components of the nanofiber mat, *i.e.* polyacrylic acid, 2,4,6-trimethoxybenzaldehyde and 1,1,1-trishydroxymethyl ethane (Fig. S7†).

We then repeated this study with doxorubicin-loaded buttresses. Supernatant from buttresses incubated at pH 7.4, as expected, showed no cytotoxicity; while, in contrast, the supernatant from buttresses incubated at pH 6.5 significantly reduced cell viability in three different human cancer cell lines, including: breast cancer (MDA-MB-231) and lung cancer (NCI-H460 and A549; Fig. 6b). We used LC-MS to quantify doxorubicin release from the buttresses and, hence, present in the treatment of these cells. The final concentration of doxorubicin in the cell culture media was found to be 0.2 μM. The resultant ~20% to 40% reduction in cell viability is consistent with the EC_{50} values for two-day treatments of doxorubicin alone (*i.e.*, free drug not loaded into a buttress) in MDA-MB-231, NCI-H460 and A549 cell lines (*i.e.*, 0.31 μM, 0.17 μM, and 0.44 μM, respectively; Fig. 6c). These results demonstrate that doxorubicin maintains its anticancer activity even after release from the buttress and, furthermore, that it is active against a variety of different cancer types.

Feasibility testing for use as a surgical buttress

To determine the feasibility of using these pH-responsive nanofiber buttresses as a reinforcing material in tumor resection surgery, we evaluated their mechanical properties using an Instron Microtester. The Young's Modulus, a measure of the tensile strength of a material, of the nanofiber buttresses was found to be 6.3 ± 1.4 MPa. For comparison, the Young's Modulus of Seamguard, a commercially available (non-drug loaded) surgical buttress used in lung and gastric resection surgeries, was measured to be 36.1 ± 4.0 MPa. While the nanofiber buttress is certainly weaker than this particular example of a commercial buttress, it is nonetheless able to function as a reinforcing material in surgical resections. To demonstrate this functionality, we performed a mock wedge resection on a porcine lung using a surgical cutting stapler to which two pieces of pH-responsive buttress were secured (Fig. 7). After

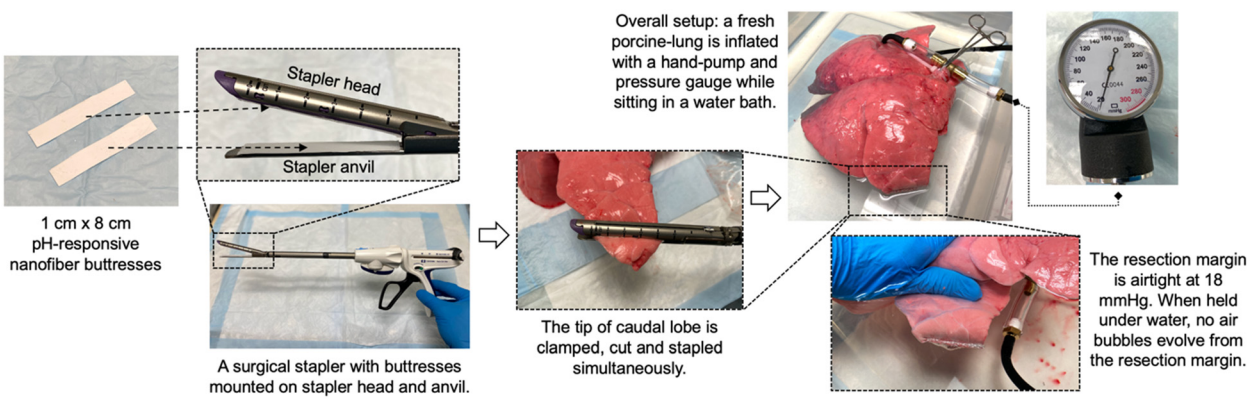

Fig. 7 Demonstration of the feasibility of using pH-responsive nanofiber buttresses as reinforcements for surgical resection margins.

resection, the lung was inflated to 18 mm Hg (25 mm H_2O), which is the standard pressure to which lungs are tested following surgical resections procedures to ensure no air leaks are present prior to the conclusion of surgery. The inflated lung was submerged in water and no bubbles evolved from the resection margin indicating a patent seal. A video demonstrating the inflation and submersion of the lung is provided in Fig. S8.† This proof-of-feasibility study demonstrates that pH-responsive nanofiber buttresses have the potential to serve as versatile medical devices that both offer mechanical reinforcement as well as localized drug delivery.

Conclusions

We describe a new pH-responsive nanofiber buttress that transforms from a hydrophobic to a hydrophilic state in the presence of mildly acidic aqueous conditions. The base polymer of the buttress contains hydrophobic acetal side chains, which are acid labile, and, upon acid-induced cleavage, reveal two hydroxyl groups on the side chain of the polymer repeat unit. This polymer is readily electrospun to afford flexible, non-woven polymer buttresses which have a cloth-like character. Contact angle measurements confirm the change in wettability of the fibers and SEM reveals an increase in fiber diameter when the buttresses are incubated under pH 5.5 or 6.5 conditions, while no changes are observed pH 7.4. As electrospinning is a versatile process, drug-loaded buttresses can be fabricated in a single synthetic step. Dye release studies at pH 5.5 and 7.4 confirmed that nanofiber buttresses with smaller diameter exhibit accelerated cargo release. While negligible passive drug release occurs at pH 7.4, a mildly acidic pH of 5.5–6.5 triggers increased drug release in a pH-dependent manner. Drug-loaded buttresses are cytotoxic to multiple human cancer cell lines. It is feasible to use these in standard lung tumor resection surgeries to reinforce the resection margin and deliver drugs locally. Future studies may explore the *in vivo* efficacy of such systems as drug delivery devices for treating diseases where a change of pH is integral to the pathology of diseases such as cancer or some inflammatory diseases.

Author contributions

I. A, S. K, A. H. C, and Y. A did the experiments. R. S., A. H. C, M. W. G., and A. S provided supervision and undertook writing of the final draft. The manuscript was written through the contributions of all authors. All authors have given approval to the final version of the manuscript.

Conflicts of interest

AHC and MWG have ownership interest in Ionic Pharmaceuticals, which has received SBIR funding to support polymer-based drug delivery technologies.

Acknowledgements

R. S acknowledges The Presidency of Republic of Turkey Directorate of Strategy and Budget for infrastructure Grant No. 2009K120520. This work was supported in part by NIH (R01CA232708 and R01CA232056) and Small Business Innovation Research (SBIR) program (2R44CA189215).

References

1 A. S. Hoffman, *Adv. Drug Delivery Rev.*, 2013, **65**, 10–16.
2 D. Roy, J. N. Cambre and B. S. Sumerlin, *Prog. Polym. Sci.*, 2010, **35**, 278–301.
3 A. Kakkar, G. Traverso, O. C. Farokhzad, R. Weissleder and R. Langer, *Nat. Rev. Chem.*, 2017, **1**, 0063.
4 X. Dong, R. K. Brahma, C. Fang and S. Q. Yao, *Chem. Sci.*, 2022, **13**, 4239–4269.
5 E. J. Falde, S. T. Yohe, Y. L. Colson and M. W. Grinstaff, *Biomaterials*, 2016, **104**, 87–103.
6 F. D. Jochum and P. Theato, *Chem. Soc. Rev.*, 2013, **42**, 7468–7483.
7 L. Chambre, L. Rosselle, A. Barras, D. Aydin, A. Loczechin, S. Gunbay, R. Sanyal, N. Skandrani, N. Metzler-Nolte, J. E. Bandow, R. Boukherroub, S. Szunerits and A. Sanyal, *ACS Appl. Mater. Interfaces*, 2020, **12**, 56805–56814.
8 L. Rosselle, A. R. Cantelmo, A. Barras, N. Skandrani, M. Pastore, D. Aydin, L. Chambre, R. Sanyal, A. Sanyal, R. Boukherroub and S. Szunerits, *Biomater. Sci.*, 2020, **8**, 5911–5919.
9 Y. Kotsuchibashi, *Polym. J.*, 2020, **52**, 681–689.
10 H. Tang, W. Zhao, J. Yu, Y. Li and C. Zhao, *Molecules*, 2018, **24**, 4.
11 J. Thévenot, H. Oliveira, O. Sandre and S. Lecommandoux, *Chem. Soc. Rev.*, 2013, **42**, 7099–7116.
12 M. Huo, J. Yuan, L. Tao and Y. Wei, *Polym. Chem.*, 2014, **5**, 1519–1528.
13 I. Altinbasak, R. Sanyal and A. Sanyal, *RSC Adv.*, 2016, **6**, 74757–74764.
14 M. Arslan, R. Sanyal and A. Sanyal, *Polym. Chem.*, 2020, **11**, 1763–1773.
15 A. S. E. Ojugo, P. M. J. McSheehy, D. J. O. McIntyre, C. McCoy, M. Stubbs, M. O. Leach, I. R. Judson and J. R. Griffiths, *NMR Biomed.*, 1999, **12**, 495–504.
16 X. Zhang, Y. Lin and R. J. Gillies, *J. Nucl. Med.*, 2010, **51**, 1167–1170.
17 V. Estrella, T. Chen, M. Lloyd, J. Wojtkowiak, H. H. Cornnell, A. Ibrahim-Hashim, K. Bailey, Y. Balagurunathan, J. M. Rothberg, B. F. Sloane, J. Johnson, R. A. Gatenby and R. J. Gillies, *Cancer Res.*, 2013, **73**, 1524–1535.
18 A. Som, S. Bloch, J. E. Ippolito and S. Achilefu, *Sci. Rep.*, 2016, **6**, 27803.
19 A. Kumar, C. Montemagno and H.-J. Choi, *Sci. Rep.*, 2017, **7**, 3059.

20 W. Gao, J. M. Chan and O. C. Farokhzad, *Mol. Pharm.*, 2010, **7**, 1913–1920.
21 R. Kilic and A. Sanyal, *Adv. Polym. Sci.*, 2020, **285**, 243–294.
22 D. Aydin, M. Arslan, A. Sanyal and R. Sanyal, *Bioconjugate Chem.*, 2017, **28**, 1443–1451.
23 P. M. Mendes, *Chem. Soc. Rev.*, 2008, **37**, 2512–2529.
24 J. Schoeller, F. Itel, K. Wuertz-Kozak, G. Fortunato and R. M. Rossi, *Polym. Rev.*, 2022, **62**, 351–399.
25 Y. Qi, H. Min, A. Mujeeb, Y. Zhang, X. Han, X. Zhao, G. J. Anderson, Y. Zhao and G. Nie, *ACS Appl. Mater. Interfaces*, 2018, **10**, 6972–6981.
26 J. A. Kaplan, R. Liu, J. D. Freedman, R. Padera, J. Schwartz, Y. L. Colson and M. W. Grinstaff, *Biomaterials*, 2016, **76**, 273–281.
27 Z. Zhang, S. Liu, Y. Qi, D. Zhou, Z. Xie, X. Jing, X. Chen and Y. Huang, *J. Controlled Release*, 2016, **235**, 125–133.
28 O. I. Kalaoglu-Altan, R. Sanyal and A. Sanyal, *ACS Appl. Polym. Mater.*, 2020, **2**, 4026–4036.
29 O. I. Kalaoglu-Altan, B. Verbraeken, K. Lava, T. N. Gevrek, R. Sanyal, T. Dargaville, K. De Clerck, R. Hoogenboom and A. Sanyal, *ACS Macro Lett.*, 2016, **5**, 676–681.
30 O. I. Kalaoglu-Altan, R. Sanyal and A. Sanyal, *Biomacromolecules*, 2015, **16**, 1590–1597.
31 O. I. Kalaoglu-Altan, R. Sanyal and A. Sanyal, *Polym. Chem.*, 2015, **6**, 3372–3381.
32 O. I. Kalaoglu-Altan, R. Sanyal and A. Sanyal, *ACS Omega*, 2019, **4**, 121–129.
33 F. L. Zhou, R. H. Gong and I. Porat, *Polym. Int.*, 2009, **58**, 331–342.
34 L. Persano, A. Camposeo, C. Tekmen and D. Pisignano, *Macromol. Mater. Eng.*, 2013, **298**, 504–520.
35 J. Hu, H. Y. Li, G. R. Williams, H. H. Yang, L. Tao and L. M. Zhu, *J. Pharm. Sci.*, 2016, **105**, 1104–1112.
36 S. Demirci, A. Celebioglu, Z. Aytac and T. Uyar, *Polym. Chem.*, 2014, **5**, 2050–2056.
37 I. Altinbasak, R. Jijie, A. Barras, B. Golba, R. Sanyal, J. Bouckaert, D. Drider, R. Bilyy, T. Dumych, S. Paryzhak, V. Vovk, R. Boukherroub, A. Sanyal and S. Szunerits, *ACS Appl. Mater. Interfaces*, 2018, **10**, 41098–41106.
38 S. T. Yohe, J. A. Kopechek, T. M. Porter, Y. L. Colson and M. W. Grinstaff, *Adv. Healthcare Mater.*, 2013, **2**, 1204–1208.
39 I. Altinbasak, M. Arslan, R. Sanyal and A. Sanyal, *Polym. Chem.*, 2020, **11**, 7603–7624.
40 S. Y. H. Abdalkarim, H. Yu, C. Wang, Y. Chen, Z. Zou, L. Han, J. Yao and K. C. Tam, *Chem. Eng. J.*, 2019, **375**, 121979.
41 B. Singh, N. Shukla, J. Kim, K. Kim and M.-H. Park, *Pharmaceutics*, 2021, **13**, 1319.
42 T. Gong, T. Liu, L. Zhang, W. Ye, X. Guo, L. Wang, L. Quan and C. Pan, *ACS Biomater. Sci. Eng.*, 2018, **4**, 240–247.
43 R. Contreras-Cáceres, L. Cabeza, G. Perazzoli, A. Díaz, J. M. López-Romero, C. Melguizo and J. Prados, *Nanomaterials*, 2019, **9**, 656.
44 W. Cui, M. Qi, X. Li, S. Huang, S. Zhou and J. Weng, *Int. J. Pharm.*, 2008, **361**, 47–55.
45 E. R. Gillies and J. M. J. Fréchet, *Bioconjugate Chem.*, 2005, **16**, 361–368.
46 V. L. Herrera, A. H. Colby, G. Al Tan, A. M. Moran, M. J. O'Brien, Y. L. Colson, N. Ruiz-Opazo and M. W. Grinstaff, *Nanomedicine*, 2016, **11**, 1001–1015.
47 A. P. Griset, J. Walpole, R. Liu, A. Gaffey, Y. L. Colson and M. W. Grinstaff, *J. Am. Chem. Soc.*, 2009, **131**, 2469–2471.
48 M. Stolzoff, I. Ekladious, A. H. Colby, Y. L. Colson, T. M. Porter and M. W. Grinstaff, *Biomacromolecules*, 2015, **16**, 1958–1966.
49 K. A. V. Zubris, R. Liu, A. Colby, M. D. Schulz, Y. L. Colson and M. W. Grinstaff, *Biomacromolecules*, 2013, **14**, 2074–2082.
50 K. A. V. Zubris, Y. L. Colson and M. W. Grinstaff, *Mol. Pharm.*, 2012, **9**, 196–200.
51 A. H. Colby, N. H. Oberlies, C. J. Pearce, V. L. M. Herrera, Y. L. Colson and M. W. Grinstaff, *Wiley Interdiscip. Rev.: Nanomed. Nanobiotechnol.*, 2017, (9), e1451.
52 A. H. Colby, S. M. Berry, A. M. Moran, K. A. Pasion, R. Liu, Y. L. Colson, N. Ruiz-Opazo, M. W. Grinstaff and V. L. M. Herrera, *ACS Nano*, 2017, **11**, 1466–1477.
53 A. H. Colby, R. Liu, M. D. Schulz, R. F. Padera, Y. L. Colson and M. W. Grinstaff, *Sci. Rep.*, 2016, **6**, 18720.
54 Y. L. Colson, R. Liu, E. B. Southard, M. D. Schulz, J. E. Wade, A. P. Griset, K. A. V. Zubris, R. F. Padera and M. W. Grinstaff, *Biomaterials*, 2011, **32**, 832–840.
55 D. Gilmore, M. Schulz, R. Liu, K. A. V. Zubris, R. F. Padera, P. J. Catalano, M. W. Grinstaff and Y. L. Colson, *Ann. Surg. Oncol.*, 2013, **20**, 1684–1693.
56 A. H. Colby, R. Liu, R. P. Doyle, A. Merting, H. Zhang, N. Savage, N. Q. Chu, B. A. Hollister, W. McCulloch, J. E. Burdette, C. J. Pearce, K. Liu, N. H. Oberlies, Y. L. Colson and M. W. Grinstaff, *J. Controlled Release*, 2021, **337**, 144–154.
57 A. H. Colby, Y. L. Colson and M. W. Grinstaff, *Nanoscale*, 2013, **5**, 3496–3504.
58 D. Hanahan and R. A. Weinberg, *Cell*, 2011, **144**, 646–674.
59 V. Estrella, T. Chen, M. Lloyd, J. Wojtkowiak, H. H. Cornnell, A. Ibrahim-Hashim, K. Bailey, Y. Balagurunathan, J. M. Rothberg, B. F. Sloane, J. Johnson, R. A. Gatenby and R. J. Gillies, *Cancer Res.*, 2013, **73**, 1524–1535.